Electronic Supplementary Material (ESI) for Journal of Materials Chemistry A.

A bioinspired strategy towards super-adsorbent hydrogel spheres via self-sacrificing micro-reactors for robust wastewater remediation

Xin Song,[a] Jiangle An,[a] Chao He,[a] Jukai Zhou,[a,b] Yuanting Xu,[a] Haifeng Ji,[a] Li Yang,[a,c] Jiarui Yin,[a] Weifeng Zhao,[a] and Changsheng Zhao [a,d**]*

[a] *College of Polymer Science and Engineering, State Key Laboratory of Polymer Materials Engineering, Sichuan University, Chengdu, 610065, People's Republic of China*

[b] *Department of Macromolecular Science and Engineering, University of Michigan, Ann Arbor, Michigan, 48109, USA*

[c] *Department of Polymer Science and Engineering, Zhejiang University, Hangzhou 310027, People's Republic of China*

[d] *National Engineering Research Centre for Biomaterials, Sichuan University, Chengdu 610064, People's Republic of China*

**Corresponding author.*

E-mail: zhaoscukth@163.com (W-F. Zhao*); zhaochsh70@163.com (C-S. Zhao**)

Tel.: +86-28-85400453; Fax: +86-28-85405402.

Experimental section

Materials

Table S1. The details of the used PES.

Information	Value
Label	Ultrason@ E 6020 P
Form	granule
Odour	odourless
Colour	white
Processing Method	injection molding
Glass Transition	225 °C
Autoignition	580-600 °C
Density	1.30-1.40 g/cm^3 (20 °C,1013 hPa)
Bulk Density	250-350 kg/m^3 (20 °C,1013 hPa)
Thermal Decomposition	>400 °C
Solubility in Water	insoluble
M_w	58,000
Viscosity	4,000 mPa·s (20 wt.%)
Moisture	1.0% (23 °C, 50% RH)
Tensile Modulus	2650 MPa (23 °C)
Tensile Stress at yield	85 MPa (23 °C)
Tensile Strain at yield	6.9% (23 °C)
Heat Distortion Temperature	207 °C
Charpy Notched	6.9 kJ/m^2 (23 °C)

Fabrication of hydrogel spheres via self-sacrificing micro-reactors

The detailed concentrations of hydrogel precursor solutions were shown in **Table S2**. The concentration of micro-reactor solution was confirmed by the self-sacrificing time of micro-reactor. Briefly, a series of micro-reactor solutions with different PES concentrations (7, 8, 9, 10, 11 and 12 wt. %) were prepared. Then 20 mL micro-reactor solution were poured into a glass petri dish and then placed on an automatic thermostat

(ME-B30D, Guangdong Shunde Mingyou Electric Co., Ltd., China). After preheating for 3 minutes, the hydrogel precursor solution was dropped into the micro-reactor solution with different concentrations using a syringe needle with the diameter of 0.15 mm at 70 °C. The time recorder was run once micro-reactors were formed simultaneously around the droplets. After the micro-reactor disappeared completely, the self-sacrificing time was recorded. The self-sacrificing time curve was obtained by plotting self-sacrificing time versus micro-reactor concentration. Moreover, hydrogel spheres with different volumes and different shapes were also prepared by this method using the proper reaction vessel.

Table S2. The compositions of hydrogel precursor solutions.

Samples	AA (g)	AMPS (g)	APS (g)	MBA (g)	DI water (g)	GO (g)
M	---	0.300	0.012	0.030	1.150	0.050
M2A1	0.256	0.044	0.012	0.030	1.150	0.050
M1A1	0.223	0.077	0.012	0.030	1.150	0.050
M1A2	0.176	0.124	0.012	0.030	1.150	0.050
A	0.300	---	0.012	0.030	1.150	0.050

Characterization of hydrogel spheres

The water uptakes of the hydrogel spheres were analyzed via a gravimetric method.[1] A certain amount of hydrogel spheres was dried in an oven at 60 °C more than 2 days to get a constant weight. Then the dried hydrogel spheres were re-immersed into DI water. Afterward, the wet hydrogel spheres were weighted at different times after gently removing excess solution with a filter paper. The digital photos of the dried and wet hydrogel spheres were also obtained. The water uptakes of the hydrogel spheres were calculated by using the following equation:[2]

$$Water\ uptake\ (g/g) = \frac{W_w - W_d}{W_d} \tag{S1}$$

where W_w (g) is the weight of hydrogel spheres at different times at wet states; W_d (g) is the weight of hydrogel spheres at dried states. Three parallel samples were applied to get a reliable value, and the results were expressed as mean ± SD (n = 3).

To investigate the mechanical properties of the hydrogel spheres, the spheres were thoroughly swollen in DI water and then applied to a universal tensile testing machine

(SANS CMT4000) with a constant speed of 2 mm/minute under a 200 kg load mechanical sensor.

In order to further study the textural properties, the hydrogel spheres were thoroughly swollen in DI water and then applied to a Texture Analyser TA. XT Plus (Stable Micro Systems Ltd., Surrey, UK). The P/36R 36-mm (diameter) Aluminum Radiused AACC Probe was used to compress the sphere and redrawn. The detailed method settings were shown in **Table S3**. Six replicate analyses were performed at room temperature for each sample, providing the same conditions for each measurement. Textural parameters like hardness, springiness, cohesiveness, gumminess and resilience were determined from the resultant force-time plots.

Table S3. The method settings of the textural analysis.

Conditions	Values
Pre-test speed	2 mm/second
Compression speed	1 mm/second
Post-test speed	1 mm/second
Compressive strain	20%
Interval time	1 second
Trigger mode	Auto
Trigger force	5 g

Furthermore, the micro-morphologies of these hydrogel spheres were obtained by scanning electron microscopy (SEM, Phenom Pure, Phenom World, Netherlands). To prepare SEM samples, the hydrogel spheres were cut off after being immersed in liquid nitrogen for 1 minute and then completely freeze-dried overnight. Afterwards, the hydrogel spheres were attached to a support and then coated with a gold layer under vacuum.

The chemical structures of the hydrogel spheres were characterized by Fourier transform infrared spectroscopy (FTIR, Nicolet 560, U.S.A.). The hydrogel spheres were completely freeze-dried, and KBr disk method was used to obtain the FTIR spectra between 650 and 4000 cm^{-1}. The thermal stabilities of the hydrogel spheres

were also characterized by using a thermogravimetric analyzer (METTLLE TOLEDO, TGA/DSC 3+, Switzerland) under a dry N_2 atmosphere from 25 to 800 °C at a heating speed of 10 °C/minute. The curves of derivative thermogravimetric analysis were derived from TGA data. To further investigate the compositions of the hydrogel spheres, the hydrogel spheres were completely freeze-dried, and then energy dispersive spectra (EDS) were obtained using a JMS-7500F SEM (JEOL, Japan). Furthermore, freeze-dried hydrogel spheres were ground into powders. Then elemental analysis (EA) of the powders was obtained through an Elemental Analyzer (Euro EA 3000), while X-ray photoelectron spectroscopy (XPS) of the powders was performed with an XSAM800 electron spectrometer (Kratos Analytical, U.K.). Additionally, rotary rheometer (Rheometer RHEOTEST RN 4.1) and two-dimensional (2D) correlation FTIR spectroscopy were also used to detect the reaction time and the interactions among functional groups of the hydrogel precursor solution.

Acid–base titration was used for the determination of ion exchange capacity (IEC) because of its directness and simplicity[3]. Several hydrogel spheres of each sample were first incubated with 0.01 mol/L NaOH and 0.01 mol/L HCl solution in turns for 3 cycles, during the process, DI water was employed in between to remove residual solution on the surface of the hydrogel spheres. Afterward, the hydrogel spheres were incubated in 0.01 mol/L NaOH and 0.01 mol/L HCl solution for extra 24 h, the volumes of the solutions were about twice the volume of the theoretical IEC from calculation, which assumed that all the functional groups could be completely protonated. Finally, the HCl solution was titrated with standard NaOH solution (0.001 mol/L). The experimental IEC was calculated as follows:

$$IEC\ (mequiv./g) = \frac{V_{HCl}N_{HCl} - V_{NaOH}N_{NaOH}}{m_{dry}} \times 1000 \quad \text{(S2)}$$

where V_{HCl} and V_{NaOH} (L) are the volumes of the solutions used for titration, N_{HCl} and N_{NaOH} (mol/L) are the concentrations of the solutions. and m_{dry} (g) is the weight of the dried hydrogel spheres.

Matrix-assisted laser desorption/ionization time-of-flight mass spectrometry (MALDI-TOF-MS) was used to evaluate the stability of the hydrogel spheres. 10 g

spheres were immersed into 50 mL trichloromethane for 15 days. Then MALDI-TOF analyses were performed on an AXIMA Performance MALDI-TOF mass spectrometer with a SCOUTMTP Ion Source (Shimadzu Biotech MALDI-MS, Japan) equipped with an N_2 laser (337 nm), grid-less ion source, and reflector design. The instrument operated at an acceleration voltage of 25 kV and a reflector voltage of 26.3 kV. DHB (10 mg/mL aqueous solution) and analyst were mixed in a 5:2 ratio, and 0.3−0.5 μL was dropped onto a steel coordinate plate. Data were collected and analyzed with Shimadzu Biotech MALDI-MS software. PES/trichloromethane solution was used as the control sample.

The N_2 adsorption-desorption isotherms of the hydrogel spheres were measured at 77 K using a surface area analyzer (BELSORP-max, BEL Japan Inc., Osaka, Japan). The parameters of specific surface area, pore distribution, pore volume and mean pore diameter were obtained based on the Brunauer-Emmett-Teller (BET) and the Barrett-Joyner-Halenda (BJH) model.

Zeta potential measurement was carried out with a Zetasizer Nano-ZS90 (Malvern Instruments Ltd., UK). The hydrogel spheres before and after adsorption of MB were freeze-dried and ground to powders. Then the hydrogel powders were dispersed to make a 1 mg/mL suspension in DI water and the pH value was adjusted (pH 12). The zeta potential measurements were carried out at 25 °C.

Batch adsorption experiments

To investigate the adsorption capacities of the hydrogel spheres for different organic dyes, 3 hydrogel spheres of each sample were put into glass bottles containing 20 mL of dye solutions with an initial concentration of 1000 μmol/L. MB and MV were chosen as the representative cationic dyes, and CR and AR were chosen as the model anionic dyes. The glass bottles containing spheres and dye solution were shaking at a speed of 200 rpm at room temperature until reaching adsorption equilibrium. Then the concentrations of dyes were confirmed by using an UV-vis spectrometer (UV-1750, Shimadzu) at the corresponding wavelength (MB: 664 nm; MV: 584 nm; CR: 497 nm; AR: 528 nm). UV-vis spectra of the dye solutions before and after adsorption were also recorded. The adsorption amounts were calculated as follows:

$$q_e = (C_0 - C_e)\, V\, M / m \quad \text{(S3)}$$

where q_e (mg/g) is the adsorption amount at equilibrium, C_0 and C_e (μmol/L) are the concentrations of the dye solutions before and after adsorption, V (L) is the volume of the dye solution, M (g/mol) is the molar mass of the dye molecule, m (mg) is the weight of the dried hydrogel spheres used.

To study the adsorption kinetics, 3 hydrogel spheres of each sample were put into glass bottles containing 20 mL of MB solutions with an initial concentration of 1000 μmol/L. Then the experiments carried out at a shaking speed of 200 rpm at room temperature. The concentrations of the MB solutions at different time intervals (0, 15, 30, 45, 60, 120, 240, 360, 480, 600, 720, 1560, 3000, 3540 and 5760 minutes) were determined and the adsorption amounts of spheres were calculated as above mentioned.

To study the effect of initial dye concentrations on the adsorption amounts of hydrogel spheres, the hydrogel spheres samples were applied to MB solutions with different initial concentrations (200, 400, 600, 800, 1000, 1500 and 2000 μmol/L). For each sample, 3 hydrogel spheres were added and the experiments were carried out as above mentioned until reaching adsorption equilibrium. Then the concentrations were determined and the adsorption amounts were calculated.

The hydrogel spheres with the maximum adsorption capability were named as super-adsorbent hydrogel spheres (SAHS). Additionally, in order to investigate the effect of pH on the adsorption amounts of SAHS, 3 SAHS were applied to MB solutions (20 mL, 1000 μmol/L) with different pH values (0, 2, 4, 7, 10, 11 and 14). Then the experiments were carried out and the adsorption amounts were calculated as above mentioned.

Acid–base titration was performed to prove the competition between H+ ions and dye molecules. Two hydrogel spheres of each sample were first washed with DI water thoroughly and then incubated in 1 mL 0.01 mol/L HCl solution for 24 h. Then the HCl solution was titrated with standard NaOH solution (0.001 mol/L). Extraction experiments were performed to demonstrate the degradation of MB molecule under strong alkaline condition. A fresh MB solution (100 μmol/L) were prepared under

strong alkaline condition and then mixed with an equal volume of toluene. The mixture solution was shaking for 5 hours, then the aqueous phase was removed and an equal volume of 0.1 M HCl was added. Digital photos and UV-visible absorption spectrum were recorded.

Results and discussion

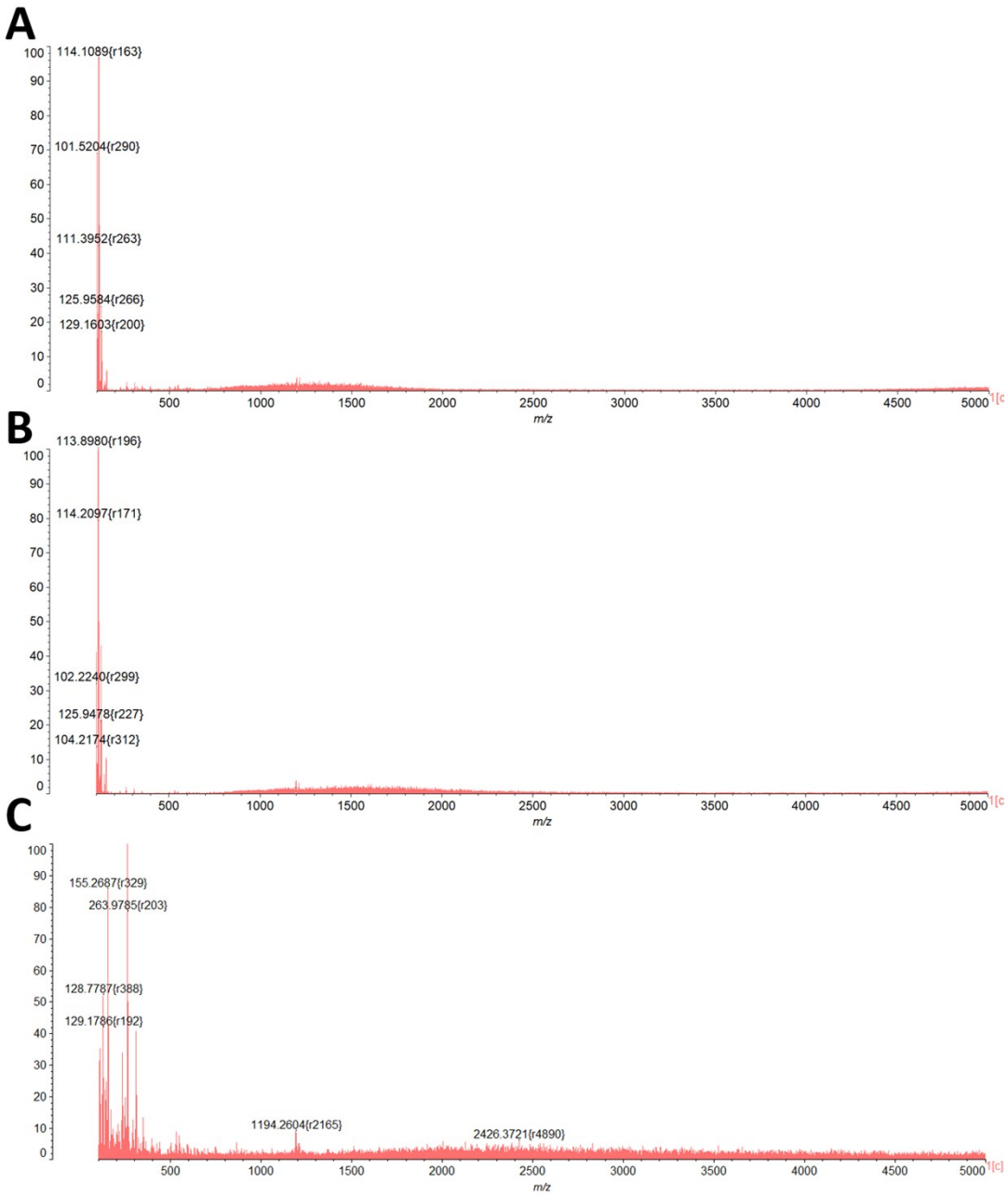

Figure S1. The MALDI-TOF-MS spectra of the trichloromethane before (A) and after incubating with the hydrogel spheres for 15 days (B) using DHB as a matrix in water. No polymer was eluted from hydrogel spheres, indicating the good stability of the hydrogel spheres. (C) The MALDI-TOF-MS spectra of the PES/trichloromethane solution. Obvious peaks of polymer could be observed, which also indicated that the micro-reactors were completely dissolved.

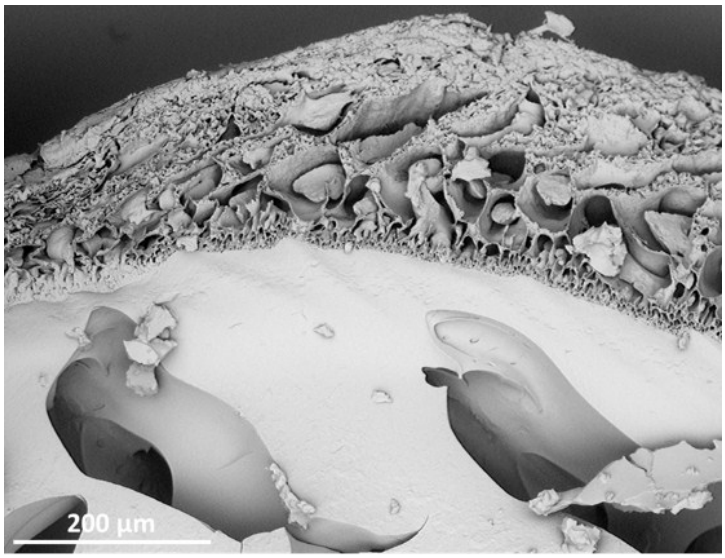

Figure S2. The cross-sectional SEM image of a hydrogel sphere with micro-reactor.

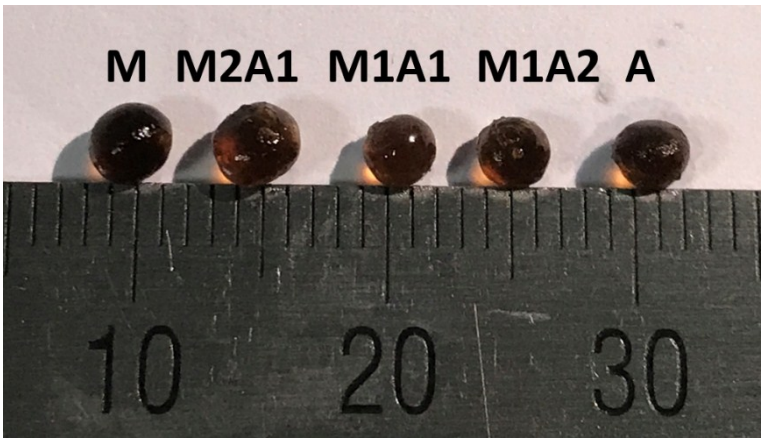

Figure S3. The digital photos of the five kinds of hydrogel spheres with different molar ratios of monomers fabricated by this strategy. The wet hydrogel spheres maintained good sphericity after cross-linking reaction and the average diameter of them were 3.06, 3.04, 2.81, 2.72 and 2.69 mm, respectively.

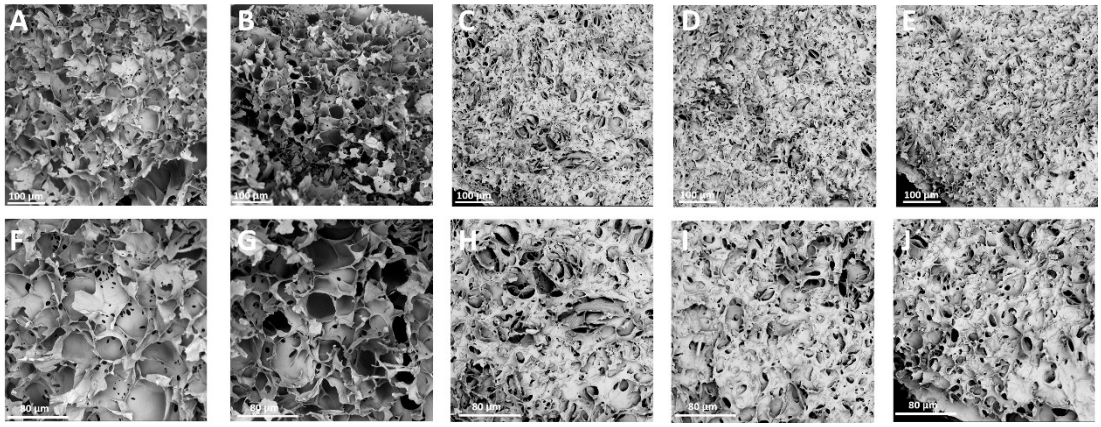

Figure S4. (A)-(E) The cross-section morphologies of the M, M2A1, M1A1, M1A2 and A at the magnification times of ×500. (F)-(J) The cross-section morphologies of the M, M2A1, M1A1, M1A2 and A at the magnification times of ×1000.

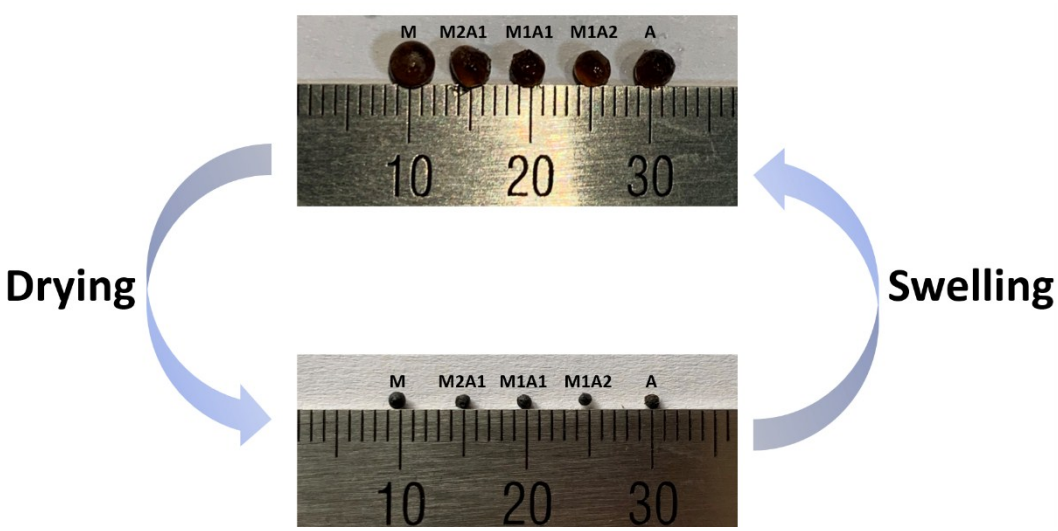

Figure S5. Digital photos of the various hydrogel spheres in wet states and in dried states. The sphericities of the spheres were maintained well in both wet and dried state, and the swelling-drying cycles could be repeated several times without breaking of spheres.

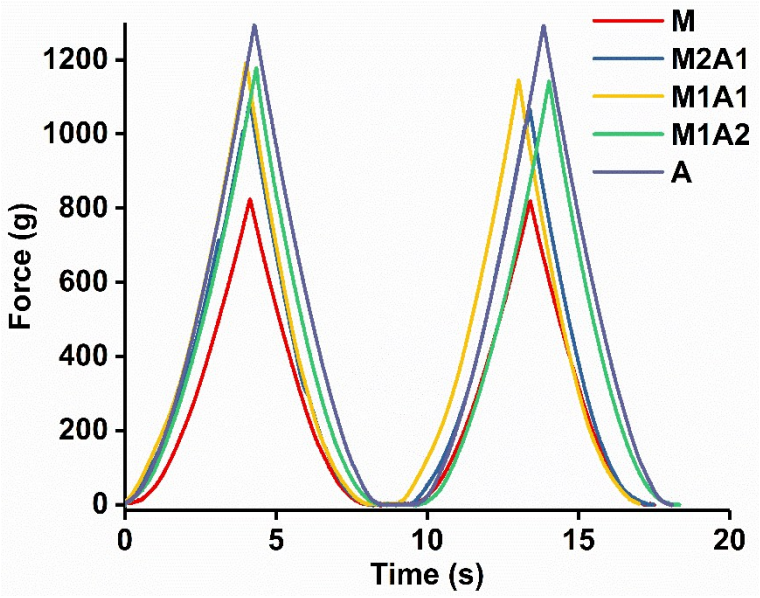

Figure S6. Typical force versus time plot of the textural measurement for the hydrogel spheres.

Table S4. The textural parameters obtained from the force-time curves. (n=6)

Samples	Textural Properties				
	Hardness	**Springiness**	**Cohesiveness**	**Gumminess**	**Resilience**
M	807.20±132.24	1.02±0.08	0.98±0.03	846.15±38.50	0.93±0.03
M2A1	1070.09±93.82	1.00±0.03	0.98±0.03	1043.74±102.50	1.22±0.77
M1A1	1163.89±52.83	0.99±0.05	0.85±0.24	1112.01±61.97	0.89±0.02
M1A2	1181.19±136.94	1.00±0.02	0.97±0.03	1155.71±149.65	1.21±0.78
A	1185.68±187.93	1.00±0.03	0.82±0.25	1156.89±245.83	0.81±0.40

Table S5. The calculated percentage compositions of C, N, O and S elements in the hydrogel spheres. Data were obtained from XPS analysis. The percentage compositions of N and S element decreased with decreasing the feed ratio of AMPS as expected.

Samples	at. conc. (%)			
	C	N	O	S
M	62.89%	7.57%	23.90%	5.64%
M2A1	63.04%	7.07%	24.67%	5.22%
M1A1	67.10%	5.58%	23.29%	4.03%
M1A2	74.68%	3.13%	20.54%	1.66%
A	75.49%	2.86%	21.65%	0.20%

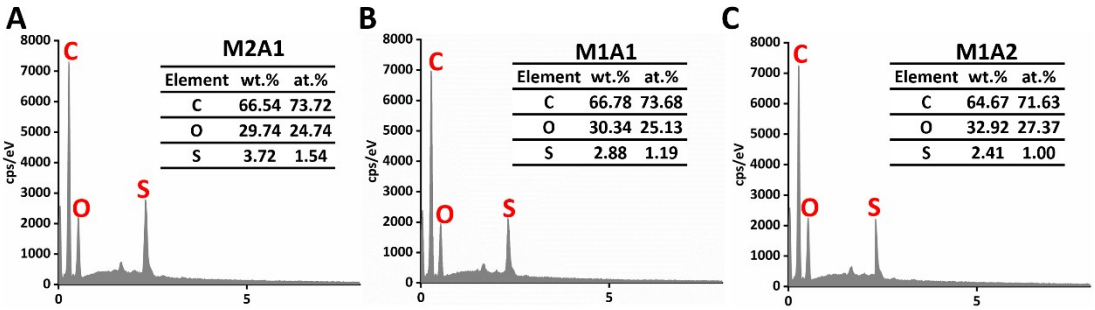

Figure S7. The EDS and calculated elemental compositions of the M2A1 (A), M1A1 (B) and M1A2 (C) hydrogel spheres.

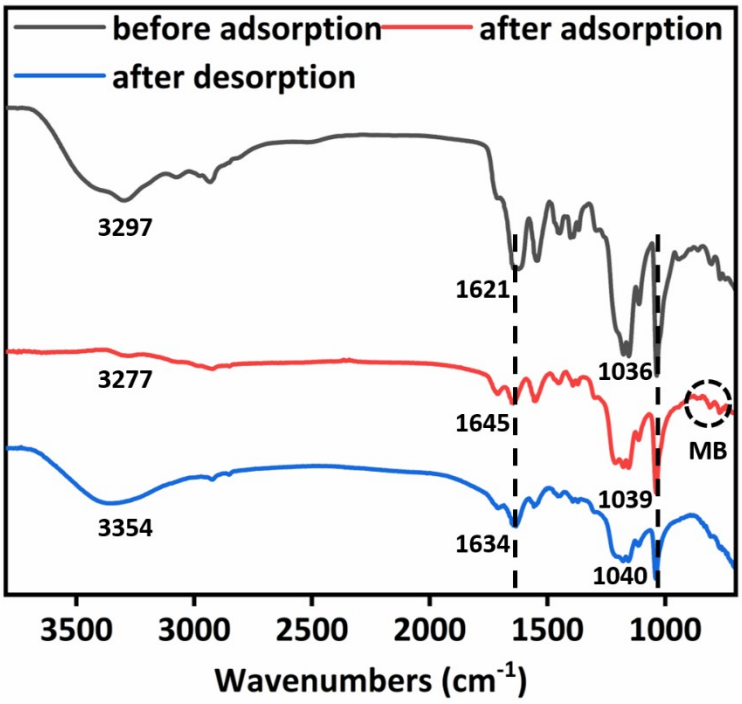

Figure S8. The FTIR spectra of SAHS before MB adsorption, after MB adsorption and after MB desorption.

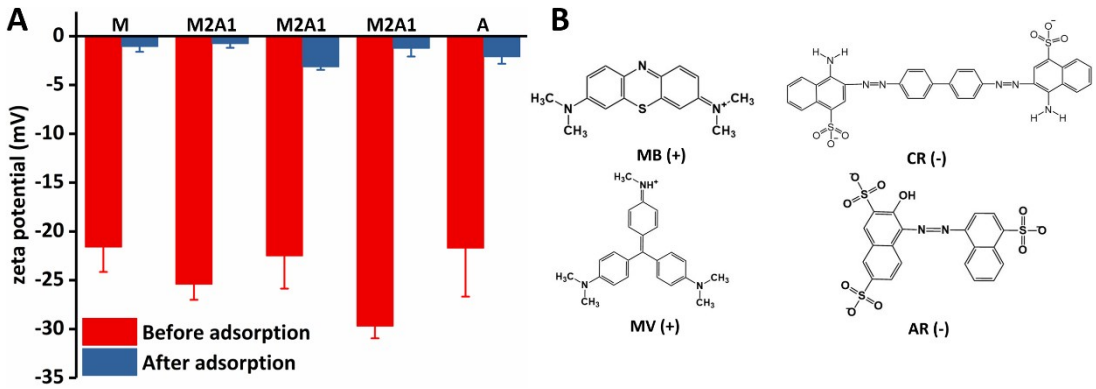

Figure S9. (A) The zeta potential of the hydrogel spheres before and after adsorption of MB. (B) The chemical structures and surface charges of MB, MV, CR and AR.

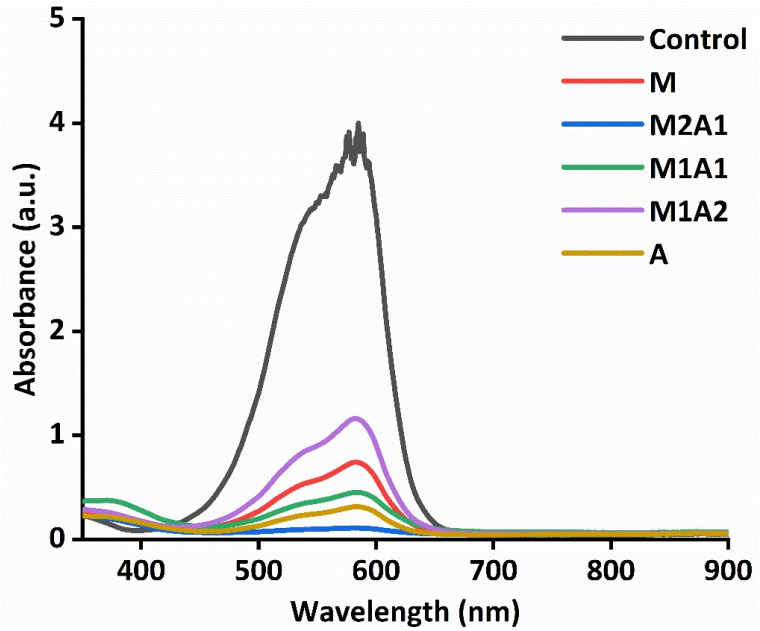

Figure S10. The variation of UV-vis spectra of the MV solutions after being adsorbed by different hydrogel spheres. (initial concentration: 1000 μmol/L; the solutions were diluted 10 times for recording the spectra).

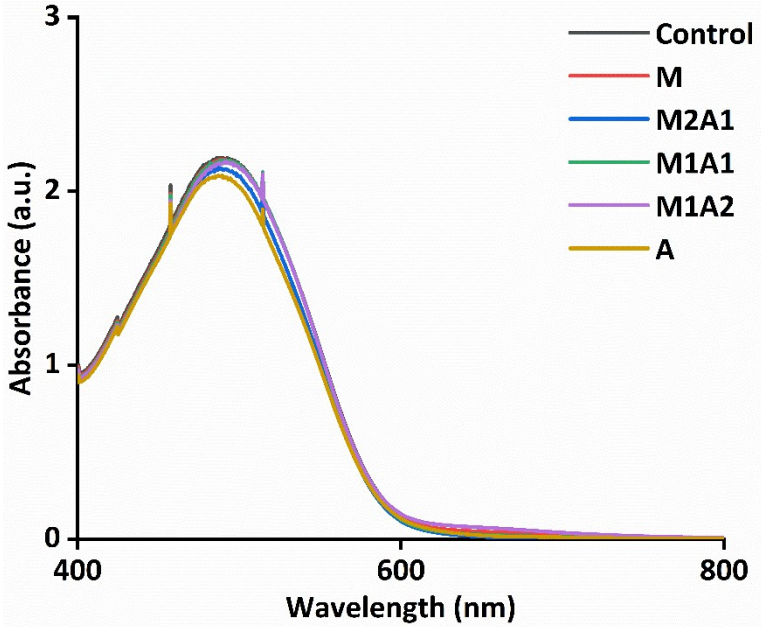

Figure S11. The variation of UV-vis spectra of the CR solutions after being adsorbed by different hydrogel spheres. (initial concentration: 1000 μmol/L).

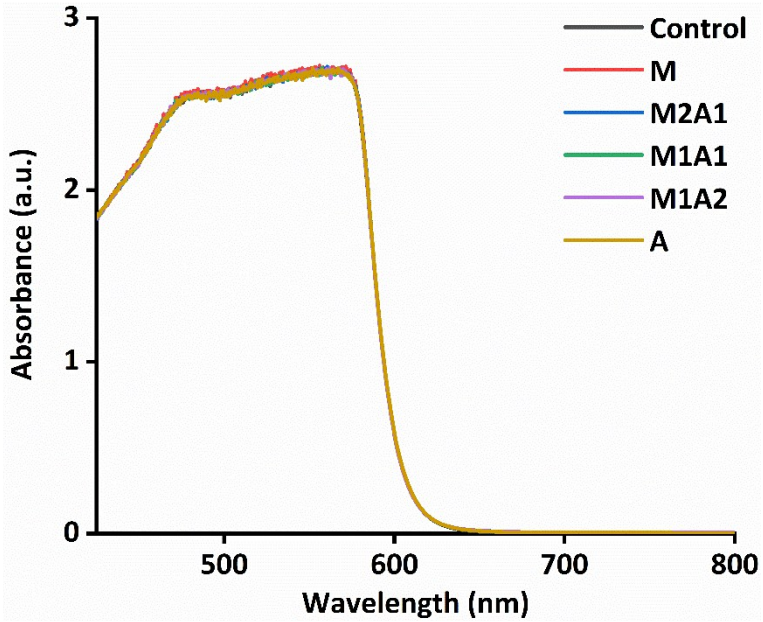

Figure S12. The variation of UV-vis spectra of the AR solutions after being adsorbed by different hydrogel spheres. (initial concentration: 1000 μmol/L).

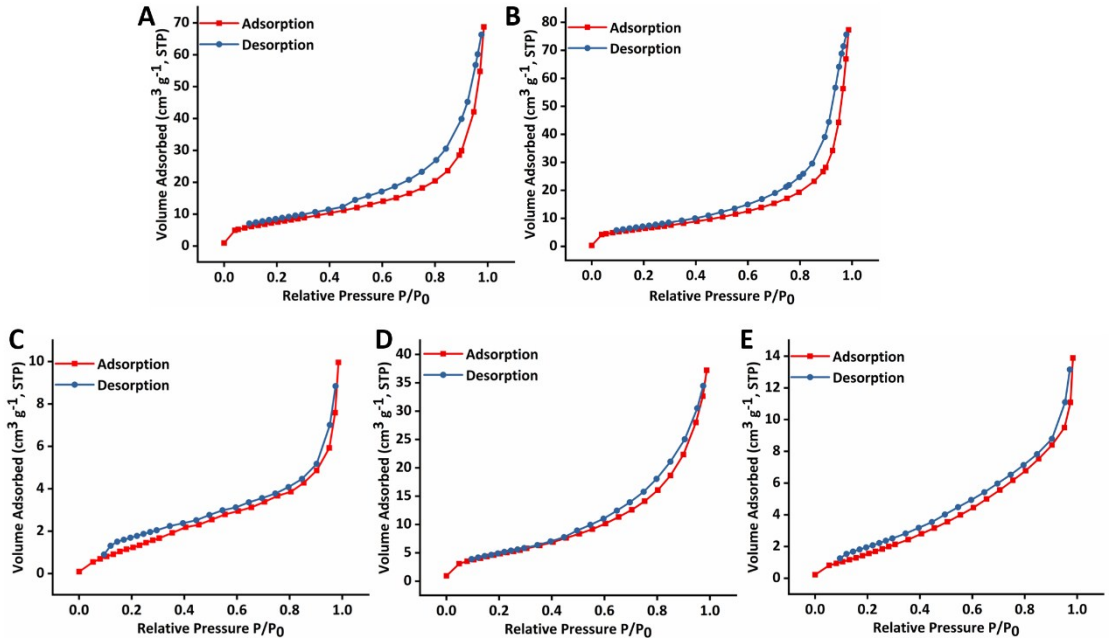

Figure S13. The N_2 adsorption-desorption isotherms for the M (A), M2A1 (B), M1A1 (C), M1A2 (D) and A (E), T= 77 K.

Table S6. The relevant parameters for M, M2A1, M1A1, M1A2 and A hydrogel spheres.

Samples	V_m (cm^3 STP g^{-1})	$a_{s,BET}$ (m^2 g^{-1})	Total Pore Volume (cm^3 g^{-1})	Mean Pore Diameter (nm)
M	6.5294	28.419	0.1063	14.965
M2A1	5.5116	23.989	0.1196	19.936
M1A1	1.4304	6.2257	0.0154	9.8946
M1A2	4.2612	18.547	0.0576	12.413
A	2.0232	8.8057	0.0215	9.7552

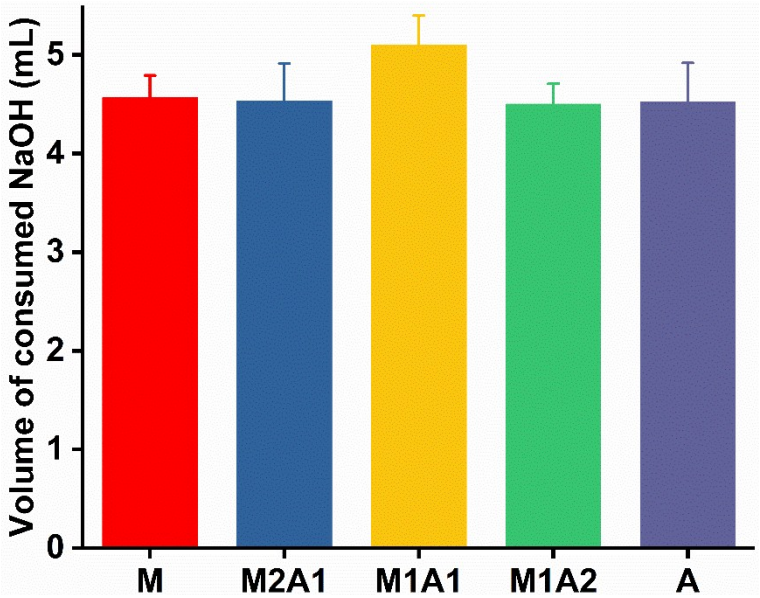

Figure S14. The volumes of consumed 0.001mol/L NaOH solution for titration of 1mL 0.01mol/L HCl after incubating with the hydrogel spheres.

Adsorption kinetic studies

Furthermore, pseudo-first-order, pseudo-second-order and intraparticle diffusion kinetic models were employed to analyze the MB adsorption process. The pseudo-first-order equation is the first-rate equation for the adsorption of liquid-solid system based on solid capacity[4] and can be expressed by the following equation:[5]

$$\ln(q_e - q_t) = \ln q_e - k_1 t \quad \text{(S4)}$$

where k_1 is the rate constant of pseudo-first-order kinetic model; q_t is the adsorption amount of MB at time t (mg/g); q_e is that adsorbed at the equilibrium (mg/g).

For the pseudo-second-order reaction, the rate depends on the adsorbed amount when the adsorption reached equilibrium and the adsorbed amount on the surface of adsorption material.[6] The equation can be written as follows:[5]

$$\frac{t}{q_t} = \frac{1}{k_2 q_e^2} + \frac{t}{q_e} \quad \text{(S5)}$$

where k_2 is the rate constant of the pseudo-second-order kinetic model; the meaning of q_t, q_e, and t are the same as those in Eq. (S4).

The intra-particle diffusion model is also used to identify the diffusion mechanism and it can be represented by the following equation:[7]

$$q_t = k_p t^{1/2} + C \quad \text{(S6)}$$

where k_p (mg/g $\text{min}^{1/2}$) and C (mg/g) are the constant of intraparticle diffusion model; the meaning of q_t is the same as that in Eq. (S4).

Table S7. The pseudo-first-order kinetic models and the parameters for the adsorption of MB to the hydrogel spheres.

Parameters	Samples				
	M	M2A1	M1A1	M1A2	A
K_1 (min^{-1})	0.0008	0.0016	0.0006	0.00104	0.0009
$Q_{e,\,cal}$ (mg/g)	2114.683	2092.783	1240.81	1903.577	1693.089
R^2	0.925	0.919	0.642	0.908	0.938

Table S8. The pseudo-second-order kinetic models and the parameters for the adsorption of MB to the hydrogel spheres.

Parameters	Samples				
	M	M2A1	M1A1	M1A2	A
$Q_{e,\,cal}$ (mg/g)	3202.948	3658.252	2578.238	3065.314	2545.066
$Q_{e,\,exp}$ (mg/g)	3240.861	3746.160	2551.912	3142.826	2608.807
K_2 (g mg^{-1} min^{-1})	1.61×10^{-6}	2.49×10^{-6}	3.33×10^{-5}	1.91×10^{-6}	2.04×10^{-6}
R^2	0.99665	0.99950	0.99728	0.99901	0.99815

Table S9. The intra-particle diffusion kinetic models and the parameters for the adsorption of MB to the hydrogel spheres.

Parameters		Samples				
		M	M2A1	M1A1	M1A2	A
Step 1	C_1	-41.9956	-87.0640	-86.2169	-102.3525	-87.4221
	k_{p1}	123.8762	150.5390	125.0487	110.8166	97.3056
	R_1^2	0.92590	0.95051	0.80817	0.86082	0.88089
Step 2	C_2	862.2919	969.7880	1229.7135	724.4371	685.1845
	k_{p2}	55.1513	92.2697	35.7877	68.9529	48.1712
	R_2^2	0.92636	0.96924	0.85091	0.97990	0.95179
Step 3	C_3	2137.6960	3471.2891	1965.7121	2568.6057	1937.6965
	k_{p3}	14.5892	2.7108	7.5932	6.8275	8.4901
	R_3^2	0.95090	0.83806	0.84677	0.94260	0.89501

Adsorption isotherm studies

The adsorption isotherms describe the interaction between absorbent and absorbate, and they are critical for optimizing the application of absorbents. Herein, Langmuir isotherm, Freundlich isotherm and Sips isotherm are applied, since they are three of the most widely used adsorption isotherms to study the adsorption of solute from liquid solutions. The Langmuir model assumes that all adsorption sites are homogeneous, the adsorption process is a dynamic balance, the adsorption occurs in monolayer, and the adsorbed molecules are all independent.[8, 9] It can be expressed as follows:

$$\frac{C_e}{q_e} = \frac{1}{q_{\max} k_L} + \frac{C_e}{q_{\max}} \tag{S7}$$

where C_e (mg/L) is the concentration of the CR at equilibrium; q_e (mg/g) is the amount of CR adsorbed by the unit mass after the adsorption reaches equilibrium; q_{max} (mg/g) is the adsorption capacity; K_L (L/mg) is the Langmuir adsorption constant.

Freundlich isotherm is an empirical equation used to describe the heterogeneous system and it depicts reversible adsorption. It can be expressed by the following equation:[10]

$$q_e = k_F C_e^{1/n} \tag{S8}$$

where $1/n$ is the constant which incorporate factors affecting the adsorbed amount at equilibrium; k_F is the Freundlich isotherm constant (mg/g) $(L/mg)^{1/n}$; the meanings of q_e (mg/g) and C_e (mg/L) are the same as those in the Langmuir equation.

The linear form of the Freundlich isotherm equation is as follows:

$$\ln q_e = k_F + (1/n) \ln C_e \tag{S9}$$

The Sips isotherm is an empirical model for representing equilibrium adsorption data.[11, 12] It is a generalization of the Langmuir and Freundlich isotherms. The equation could be represented as follows:[13]

$$q_e = \frac{q_{m_s} k_s C_e^{m_s}}{1 + k_s C_e^{m_s}} \tag{S10}$$

where m_S is the Sips model exponent; k_S is the Sips equilibrium constant $(L/mg)^m$; q_{ms} (mg/g) is the Sips maximum adsorption capacity. The meanings of q_e (mg/g) and C_e

(mg/L) are the same as those in the Langmuir equation.

Table S10. The Langmuir isotherm models and the parameters for the adsorption of MB to the hydrogel spheres.

Parameters	Samples				
	M	M2A1	M1A1	M1A2	A
Q_{max} (mg/g)	6867.094	8232.147	3966.129	4753.846	4489.479
K_L (L/mg)	0.00204	0.00182	0.00422	0.00352	0.00272
R^2_L	0.98754	0.99069	0.99130	0.98542	0.98477

Table S11. The Freundlich isotherm models and the parameters for the adsorption of MB to the hydrogel spheres.

Parameters	Samples				
	M	M2A1	M1A1	M1A2	A
n	1.50042	1.44814	1.92600	1.79485	1.66472
k_F (mg/g) $(L/mg)^{1/n}$	4.00929	3.9823	4.68162	4.56308	4.12499
R^2_F	0.98197	0.98473	0.95127	0.95872	0.97624

Table S12. The Sips isotherm models and the parameters for the adsorption of MB to the hydrogel spheres.

Parameters	Samples				
	M	M2A1	M1A1	M1A2	A
q_{ms} (mg/g)	6049.7025	7110.5885	3493.8917	4125.3353	4030.2103
k_S (L/mg)^m	0.00135	0.00122	0.00145	0.00128	0.00158
m_S	1.11333	1.11611	1.25450	1.24466	1.13592
R^2_S	0.99452	0.99684	0.99132	0.98689	0.98927

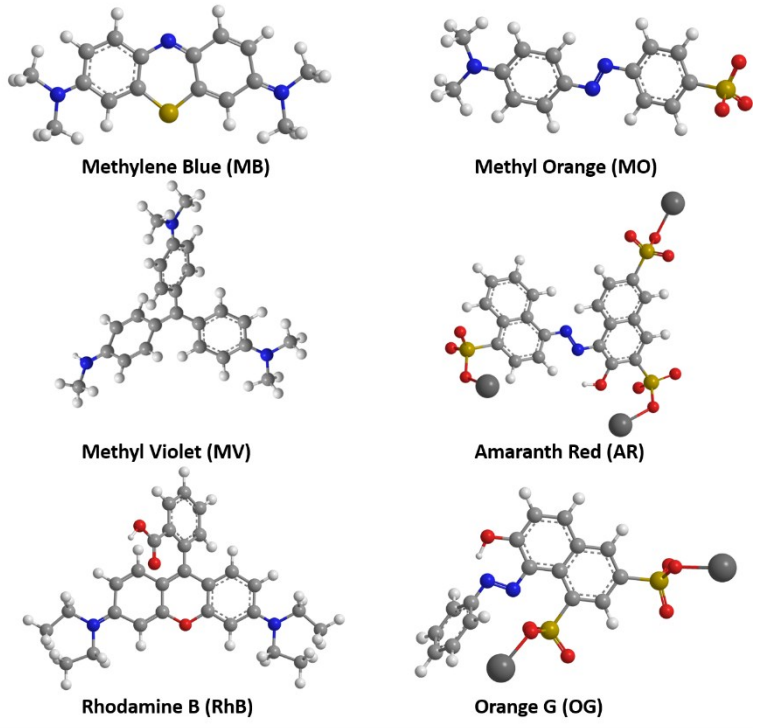

Figure S15. The chemical structures of the dye molecules.

Table S13. The hydration diameters, hydration enthalpies, ionic potential, electronegativity and relative atomic mass of the heavy metallic ions.

Characteristics	Heavy metallic ions			
	Ni^{2+}	Cu^{2+}	Ag^{+}	Pb^{2+}
Hydration radii (Å)	4.04	4.19	3.41	4.01
Hydration enthalpies (kJ mol^{-1})	-1980	-2010	-430	-1425
Ionic potential	3.0	2.8	0.89	3.3
Electronegativity	1.91	1.9	1.93	2.33
Relative atomic mass	58.69	63.55	107.86	207.20

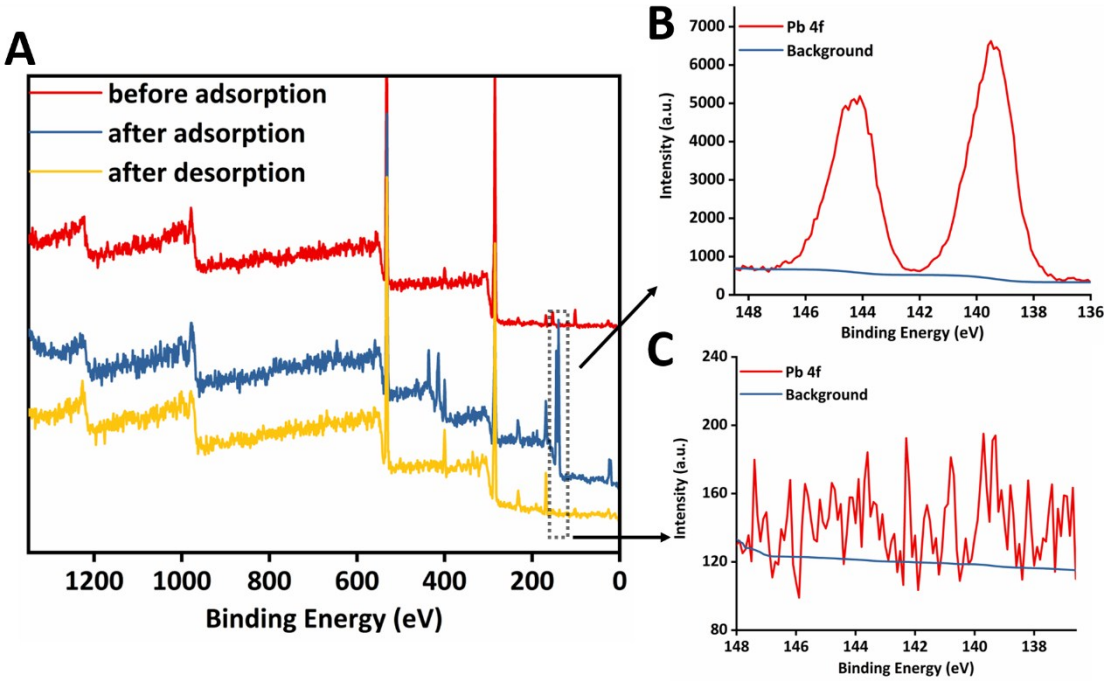

Figure S16. (A) The XPS wide spectra of the SAHS before Pb^{2+} adsorption, after Pb^{2+} adsorption and after Pb^{2+} desorption. The Pb 4f spectra of the SAHS after Pb^{2+} adsorption (B) and after Pb^{2+} desorption (C).

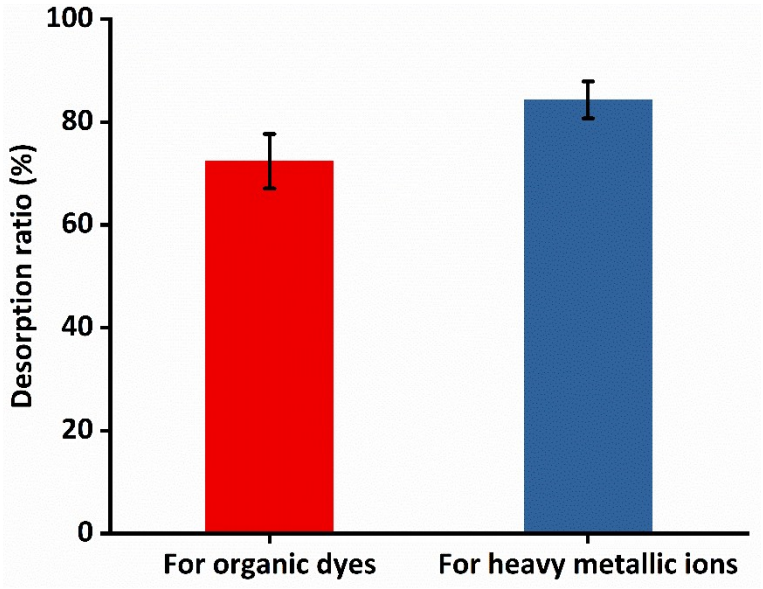

Figure S17. The desorption ratios for organic dyes (MB as the representative) by NaCl solution (1 mol/L) and for heavy metallic ions (Pb^{2+} as the representative) by EDTA solution (1 mol/L).

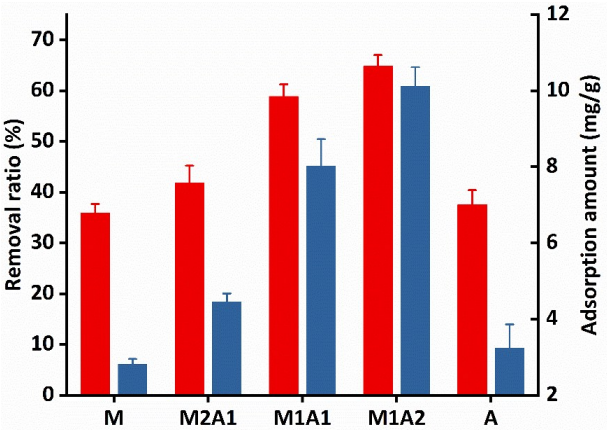

Figure S18. The removal ratios (the left axis) and the adsorption amounts (the right axis) of the hydrogel spheres for Cr (VI).

References

1. X. L. Huang, R. Wang, T. Lu, D. X. Zhou, W. F. Zhao, S. D. Sun and C. S. Zhao, *Biomacromolecules*, 2016, **17**, 4011-4020.
2. W. Zhao, L. Glavas, K. Odelius, U. Edlund and A.-C. Albertsson, *Chemistry of Materials*, 2014, **26**, 4265-4273.
3. E. Moukheiber, G. De Moor, L. Flandin and C. Bas, *Journal of membrane science*, 2012, **389**, 294-304.
4. Y. S. Ho and G. McKay, *Water Research*, 1999, **33**, 578-584.
5. S. Sen Gupta and K. G. Bhattacharyya, *Journal of Hazardous Materials*, 2006, **128**, 247-257.
6. M. Dogan, Y. Ozdemir and M. Alkan, *Dyes and Pigments*, 2007, **75**, 701-713.
7. X. Y. Yang and B. Al-Duri, *Journal of Colloid and Interface Science*, 2005, **287**, 25-34.
8. C. Namasivayam and D. Kavitha, *Dyes and Pigments*, 2002, **54**, 47-58.
9. Y. Yao, F. Xu, M. Chen, Z. Xu and Z. Zhu, *Bioresource Technology*, 2010, **101**, 3040-3046.
10. B. L. Xia, G. L. Zhang and F. B. Zhang, *Journal of Membrane Science*, 2003, **226**, 9-20.
11. R. Sips, *Journal of Chemical Physics*, 1948, **16**, 490-495.
12. S. Al-Asheh, F. Banat, R. Al-Omari and Z. Duvnjak, *Chemosphere*, 2000, **41**, 659-665.
13. O. Hamdaoui and E. Naffrechoux, *Journal of Hazardous Materials*, 2007, **147**, 401-411.